II International Conference on Simulation for Additive Manufacturing - Sim-AM 2019
F. Auricchio, E. Rank, P. Steinmann, S. Kollmannsberger and S. Morganti (Eds)

DESIGNING ADDITIVELY MANUFACTURED PARTS VIA TOPOLOGY OPTIMIZATION - A SPACE INDUSTRY CASE STUDY

B. Barroqueiro[1,2,*], A. Andrade-Campos[1] and R.A.F. Valente[1]

[1] Department of Mechanical Engineering, Centre for Mechanical Technology & Automation, University of Aveiro, 3810-193 Aveiro, Portugal.

[2] Active Space Technologies, Actividades Aeroespaciais S.A., Parque Industrial de Taveiro, Lote12, 3045-508 Coimbra, Portugal.

[*] Corresponding Author: B. Barroqueiro (bjfb@ua.pt)

Key words: Topology Optimization; Additive Manufacturing; Case Study; Space Industry;

Abstract. Additive Manufacturing (AM) allows unprecedented design freedom, which can be explored by the Topology Optimization (TO) algorithm. Their interplay allows a new engineering cycle with the potential to design and manufacture disruptive concepts. Thus, a systematic methodology for designing AM parts is presented, being the main goal of this study. The methodology is subdivided into several phases, each phase contains several tasks. Moreover, the data flow between phases is considered and solutions are provided. Finally, the methodology is applied to a space case study and preliminary results of the AM engineering cycle (TO, part design and structural analysis) are depicted.

1 INTRODUCTION

"Additive Manufacturing (AM) is a process of joining bulk raw materials to make parts from 3D model data, usually layer upon layer, as opposed to subtractive manufacturing and formative methodologies. It is an inherent part of the parts development or production process. It is used to manufacture prototypes and production parts" [1]. Moreover, this process provides great geometrical freedom and the tools to explore the referred freedom are needed. The search-optimal material layout can be performed by Topology Optimization (TO) and its interplay with AM has proven to be advantageous [2]. In the space industry, there are successful examples, where the interplay of TO and AM allow the reduction of the number of parts, assembling operations, mass and, therefore, cost (*e.g.* [3, 4]). Beyond that, the new technology opens a new dimension of design solutions by overcoming the restrictions of conventional manufacturing processes. The adopted engineering cycle consists in topology optimization (*e.g.* MSC Nastran® tool for an initial design), manual CAD[1] construction (*e.g.* CATIA V5®), structural analysis and production (process preparation and manufacturing). However, manual CAD reconstruction is ineffective. In the one hand, TO commonly produces complex geometries that are labour intensive to reproduce in CAD software. On the other hand, the TO design can be simplified in

[1] Computer Aided Design

order to allow a rapid CAD model construction with a performance cost. Thus, in this work, the presented methodology proposes an alternative methodology to the manual CAD model construction, which allows for a quicker engineering cycle. Moreover, this paper proposes a systematic methodology of a complete engineering cycle for space AM part. Furthermore, a space case study is presented, where the topology optimization, part design and structural analysis are presented and discussed. Finally, the main goal of this article is the methodology systematization for designing AM parts. Therefore, this work can provide valuable guidance for new engineers working in this field.

2 Methodologies

The complete engineering cycle of AM structures involves numerous steps. Figure 1 depicts the whole process of designing structures within framework subsystems structures of the space industry. For the sake of clarity, the process is illustrated as a linear flow, but iterative work between steps is expected to originate a non-linear flow.

2.1 Topology optimization

Topology optimization is a type of structural optimization that seeks the optimum material layout [5]. Within the scope of this work, solver 200 from MSC Software [6] was used to perform the Topology Optimization (TO) analysis, considering compliance minimization with a volume constraint. The referred solver uses the well known Solid Isotropic Material with Penalization (SIMP) method and the process starts with initial domain definition [6, 7]. Within the scope of this work, the domain is meshed using isoparametric `HEX8` elements. The mesher is available on a Patran utility named *Regular Cube Mesher 2*. After application of the boundary conditions, objective, constraint and design/non-design domains definition, the optimization cycle can start. After convergence, the resultant material distribution would ideally be a binary distribution (void or solid material) across the design domain. However, the SIMP model uses a continuous function and some intermediate densities may remain after convergence. These intermediate densities have to become either void (zero) or solid (one) and, thus, the user has to define the threshold. At the end, all solid elements become the optimized topology. Using the referred topology, the skin elements are extracted using the utility named *Skin Solid Elements*. Then, the resultant `QUAD` elements are broken into `TRIA` elements and the surface STL mesh is exported using the export STL utility.

2.2 Smoothing and Part Edition

The smoothing operation can be done within Patran® with limited options. Within the scope of this work, the Netfabb® from Autodesk® is used to perform all the smoothing, remeshing and repair operations. The translation between the surface STL mesh to a volume `TET` mesh is not possible in Netfabb neither in Patran. The free software named GMSH [8], is used to make the referred translation, being a straightforward procedure[2]. A Nastran input file is a GMSH output, which can be imported in Patran.

[2]GMSH list of instructions: File>Merge>*.STL; Geometry>Add>Volume; Mesh>3D; File>Export>*.bdf

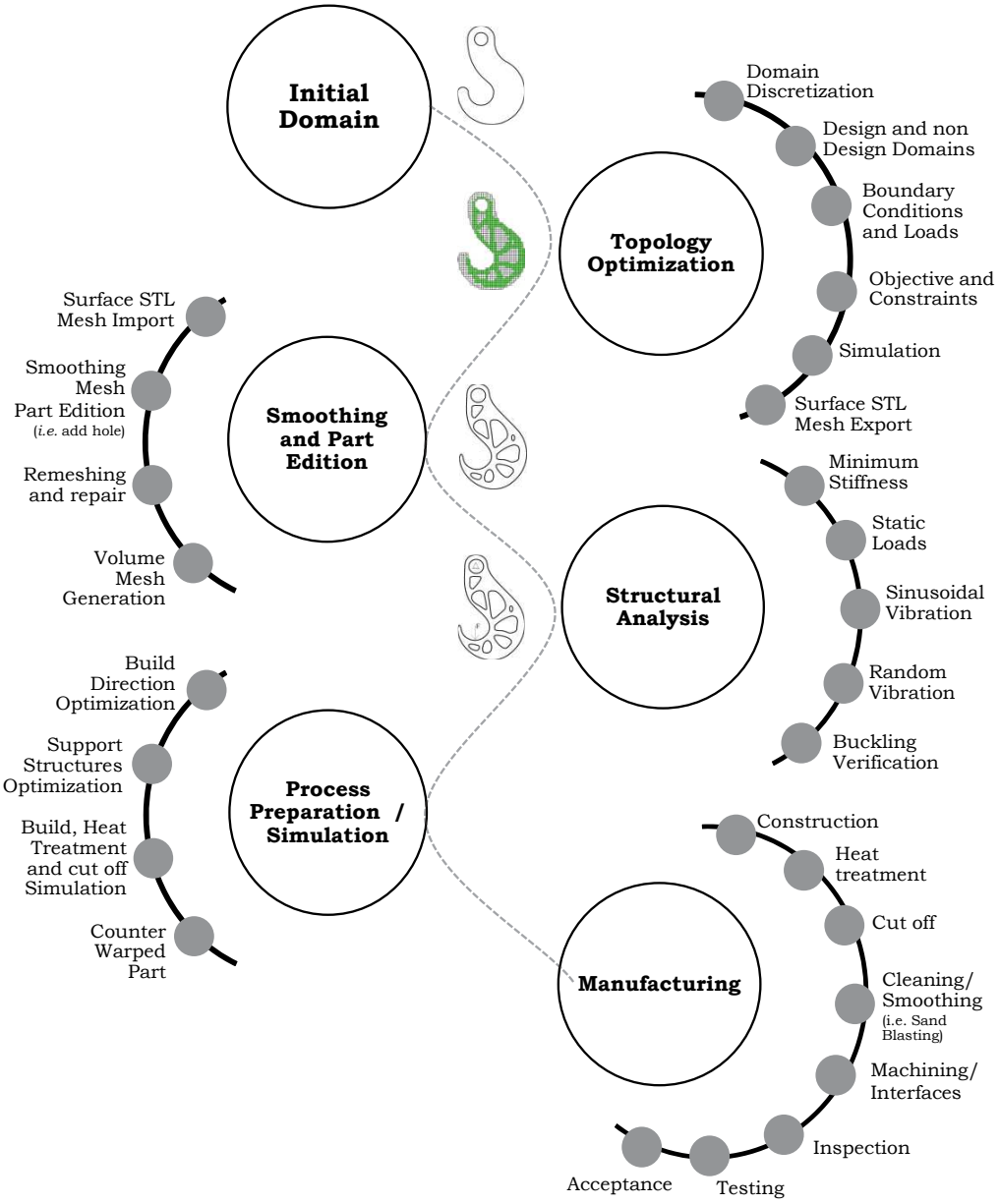

Figure 1: Engineering cycle of AM structures for the space industry.

2.3 Structural Analysis

In the space industry, the structural analysis involves at least static loads, minimum stiffness and sinusoidal/random vibration loads. Due to the typical slenderness of the designs, buckling verification is also performed. The static loads are analysed with MSC Nastran solver 101 using inertial loads [9]. The minimum stiffness requirement is verified using the MSC Nastran

solver 103 (normal modes analysis) [10], where the first eigenvalue should be above a defined limit. The sinusoidal vibration analysis is verified using the MSC Nastran modal solver 111 (Lanczos solver: frequency response) [10], considering modal damping. The random vibration is a two-step analysis. First, the frequency response analysis is performed for sinusoidal loading conditions at a sequence of frequencies. Typically, these loads are chosen to be unit loads. Thus, the output response works as a transfer function. The second step uses the referred function in order to compute the amplified random response. A quality factor of 400, a 3σ analysis and a log-log integration are considered. Additionally, the load levels are quantified in terms of Power Spectral Densities (G^2/Hz) [10]. Finally, the buckling verification is performed with MSC Nastran solver 105 using equivalent inertial loads derived the most severe load case [9].

2.4 Process Preparation and Simulation

The process preparation can be performed with some software such as Netfabb®. The first step is the optimization of the build direction, where several orientations are considered and classified in terms of different criteria (*e.g.* ratio between area and volume of support structures and/or height and volume of the build). The second step is the support structures generation, which can be generated by different available algorithms. Finally, the simulation of the build layer by layer can be also simulated in order to predict residual stress, distortions and some defects such as support structures failure or recoater interference or hot/cold spots. For instance, the Simulation Utility for Netfabb can be allegedly used to make such predictions [11]. Moreover, the software also performs the stress relief (viscoplastic analysis) and part response to the cut-off from the base. This integrated procedure allows the prediction of the part total distortion and excessive distortion on the part may lead to failure of dimensional tolerances. Thus, the process simulation can be used to apply a negative distortion on the part in order to minimize distortions and overbuild.

2.5 Manufacturing

The manufacturing stage shall start with the slicing operation of the prepared part and the G-Code generation, which can be performed in Netfabb, for example. After construction, the part shall be stress relieved, in order to decrease residual stress. Then, the part can be cut off from the baseplate and the cleaning/smoothing process (*e.g.* sandblasting) can be performed. The interfaces with tight tolerances are typically machined. Regarding quality control, the non-destructive inspection campaign can take advantage of methods such as computed tomography, eddy current testing, infrared thermography, neutron diffraction and ultrasonic testing [12]. Finally, the testing campaign involves static, sinusoidal and random testing, where the structure shall survive without deterioration. The deterioration detection can be performed with a low-intensity sinusoidal vibration sweep before and after each vibration test. If the response curve of the low-intensity sine sweeps (before and after each vibration test) are identical, no major structural deterioration will occur. The success criteria can be defined by a maximum shift of 5% and 20% for frequency and amplitude, respectively [13].

3 Case Study

The structure responsible for supporting the lens for a space instrument is analysed, named as Large Lens Mount (LLM). Titanium alloy (TI6Al4V) shall be its manufacturing material and I/F to its supporting structure is composed of six bolted connections. This use case was derived from a use case of OHB Sytems at Oberpfaffenhofen.

3.1 Topology Optimization and Smoothing

The design domain was discretised with linear isoparametric `HEX8` elements and the transition between the solid elements and the bolted connection centre point is modelled with rigid connection (RBE2). The connection between the lens (reduced to a point element) and the solid elements are modelled with RBE3, where the master nodes of volume mesh connects to a slave node on the len's CoG location (see Sub-figure 2(a)). The RBE2 element was not used, because it adds stiffness to the model. In fact, the interface region of the lens would become rigid and the TO algorithm would take advantage of the referred fact, leaving the interface poorly reinforced or the user would add to include it in the non-design domain (defeating the propose of the TO algorithm). Regarding loading conditions, the acceleration levels were replaced by an equivalent force on the len's node. Finally, the TO was performed and its objective function consists in the compliance minimization of the LLM structure, when loaded in directions X, Y and Z (weighted sum of three static load cases).

Sub-figures 2(b), 2(d), 2(f) and 2(h) describe the TO results for the volume constraints of 40%, 20%, 10% and 5%, respectively. Sub-figures 2(c), 2(e), 2(g) and 2(i) show the resultant smooth surface mesh after smoothing in Netfabb. Preliminary analysis on the designs of Sub-figures 2(c) and 2(e) revealed a design overestimation for the considered loading conditions. On the other hand, a visual inspection of the design of the Sub-figure 2(i) indicates high level of risk from the manufacturing point of view. For instance, the removal of referred support structures could lead to fracture of the thin members of the referred part. Therefore, the design of the Sub-figure 2(g) was selected and it weights 0.628 kg, which is compliant with the mass requirement. In order to facilitate the previous assessment, the model of the Sub-figures 2(g) and 2(i) were prototyped in PLA for part visualization proposes only. The Figure 3 illustrates the referred prototypes.

3.2 Structural Analysis

The design domain, Sub-figure 2(g), was discretised with isoparametric `TET10` quadratic elements [9] and the transition between the solid elements and the bolted connection center point is modelled with a rigid connection (RBE2). The connection between the lens and the volume mesh is modelled as RBE2 and the lens is modelled as a lumped mass (see Sub-figure 4(a)). In contrast with the TO analysis, the structural analysis uses RBE2, since the lens adds some stiffness and the main goal is a correct distribution of stress maps.

Table 1 lists the first ten eigenvalues of the LLM with its modal effective mass fraction for the translation (`TX`, `TY`, `TZ`) and rotational (`RX`, `RY`, `RZ`) degrees of freedom. . Within the scope of this work, only the first three modes are in excitation range and, thus, only these are

considered in analysis of the LLM. It should be noted the relevant level of coupling between the first three modes, meaning that an excitation in a given axis is likely to activate all modes in excitation range. The sine vibration excitation range (up to 100 Hz with 47 G in plane and 36 G out of plane) are far from the first eigenvalue (1461.9 Hz) and, thus, the sinusoidal vibrational analysis should be approximated to a static analysis since no relevant dynamic amplification is foreseen. The random vibration is likely to activate the first three modes and, thus, their dynamic amplification should be estimated. The direct responses for the X, Y and Z directions are shown in Sub-figures 5(a) and 5(b), considering the lens node as the monitoring point and quality factor of 400. As expected, all three modes appear in the excitation directions and their magnitude is directly related to their modal effective mass fraction.

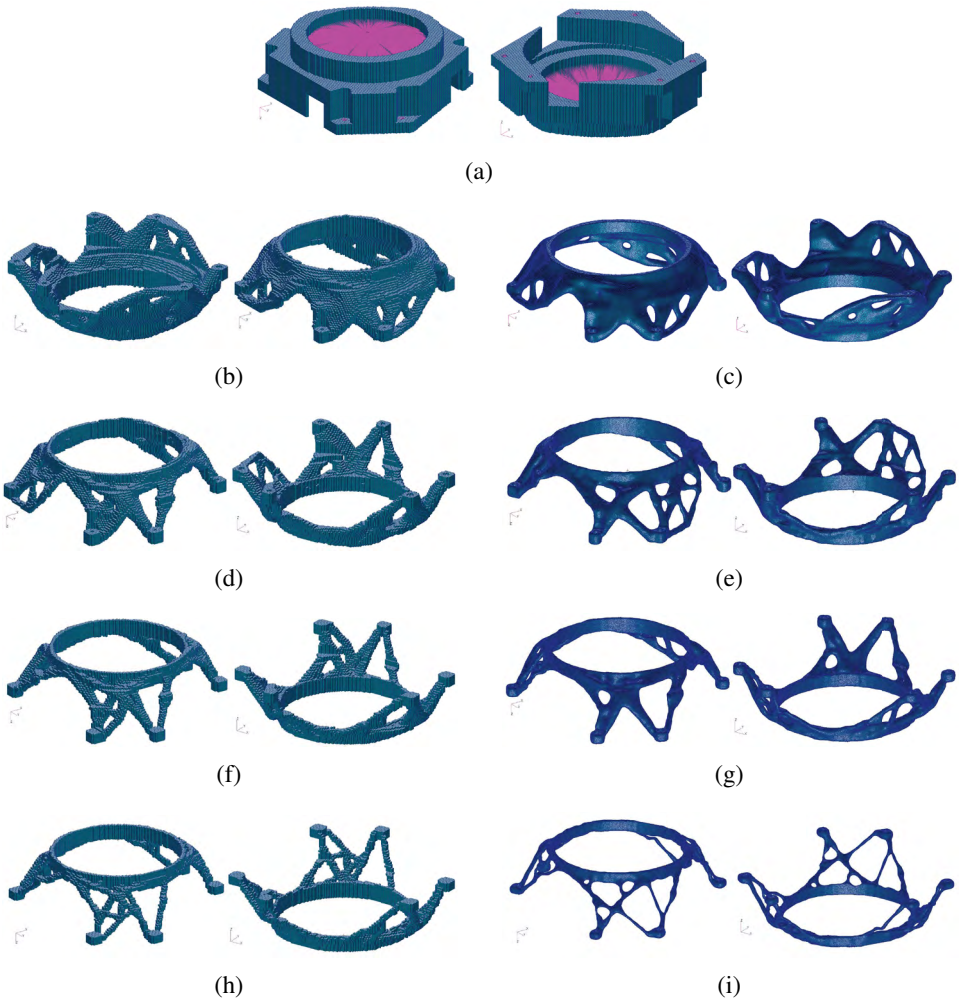

Figure 2: Discretisation of design domain in Sub-figure (a). Sub-figures (b), (d), (f) and (h) are topology optimisation results for 40%, 20%, 10% and 5% of volume fractions, respectively. Sub-figures (c), (e), (g) and (i) depicts the smooth surface meshes of the respective volume fractions.

(a) (b) (c) (d)

Figure 3: The LLM physical model printed in a dummy material (PLA). Sub-figures (a) and (b) are the design resultant from 5% of volume constraint, while Sub-figures (c) and (d) are the design resultant from 10% of volume constraint.

Table 1: List of the first ten eigenvalues of the LLM with its modal effective mass fraction for the translation.

Mode	Frequency (Hz)	TX	TY	TZ	RX	RY	RZ
1	1461.9	0.134	0.762	0.034	0.036	0.038	0.615
2	1580.0	0.757	0.152	0.014	0.014	0.009	0.178
3	1913.3	0.039	0.018	0.731	0.640	0.650	0.045
4	3142.8	0.003	0.003	0.018	0.036	0.010	0.001
5	3303.0	0.008	0.005	0.000	0.000	0.013	0.013
6	3447.1	0.000	0.006	0.003	0.000	0.001	0.001
7	3920.5	0.003	0.000	0.006	0.016	0.008	0.000
8	4173.8	0.002	0.001	0.002	0.030	0.000	0.001
9	4401.5	0.000	0.000	0.003	0.001	0.001	0.059
10	4641.9	0.001	0.001	0.039	0.002	0.009	0.008

Sub-figures 4(b), 4(d) and 4(f) depicts modal shapes of the first three eigenvalues values of the LLM. While, Sub-figures 4(c), 4(e) and 4(g) describe the static stress levels (von Mises) from the sinusoidal vibration loads and Sub-figures 4(h), 4(j) and 4(l) depict the Root Mean Square (RMS) of the stress levels (von Mises) from the random vibration loads. Due to the slenderness of the structure, buckling analysis are also presented and its inputs loads were derived from random vibration analysis. Each load case of the random vibration analysis originates a buckling load case, where the indirect and direct responses are used to compute equivalent quasi-static accelerations. The buckling stability factor is presented in Sub-figures 4(i), 4(k) and 4(m).

The minimum stiffness requirement is reached with the first eigenvalue at 1461.9 Hz when compared with 400 Hz requirement. The geometrical stability (buckling) has a relevant positive margin. The stability factor (MSC Nastran result output) should be superior to one, otherwise, the solver is predicting failure. The current design of LLM has a stability factor of 2560.9 ([3]).

Regarding strength margins, the yield stress of the Ti6Al4V should be at least 825 MPa [14] and the maximum stress levels expected from the analysis is 40 MPa, leaving the margin for further optimization (in theory). However, due to manufacturing risk, the compliance minimization with a lower volume fraction constraint (see Sub-figure 2(i)) is not used.

[3]If the factor was dangerously closer to one, a knock-down factor analysis needed to be performed due to analysis uncertainty.

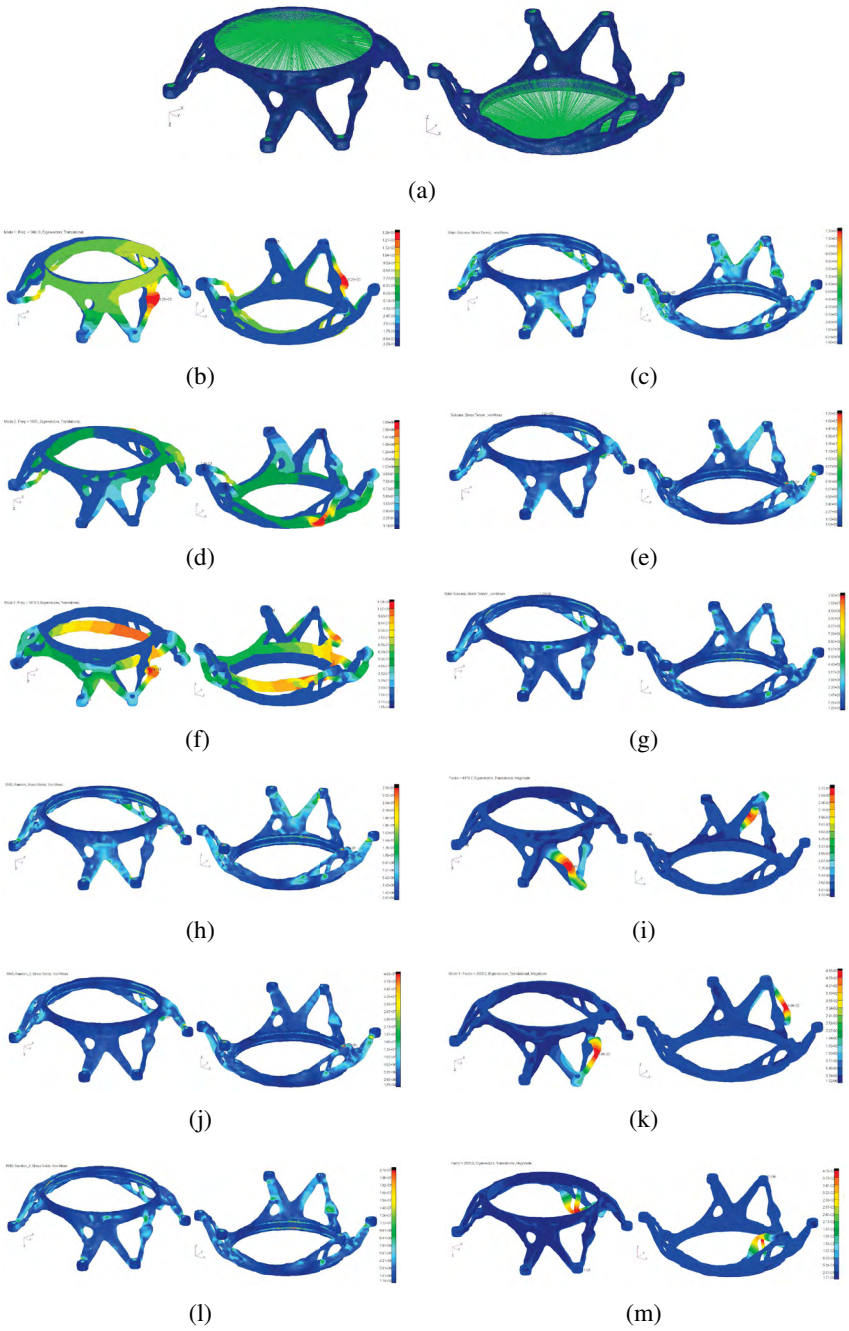

Figure 4: (a) FE modal analysis of the optimized LLM. Sub-figures (b), (d) and (f) are the modal shapes of first three eigenvalues. (c), (e) and (g) are the static von Mises stress maps when loaded in direction X, Y and Z, respectively. Sub-figures (h), (j) and (l) are the von Mises RMS values of the random vibration when exited in X, Y and Z directions, respectively. Sub-figures (i), (k) and (m) are the first buckling mode when loaded in directions X, Y and Z, respectively. All stress maps are in Pa.

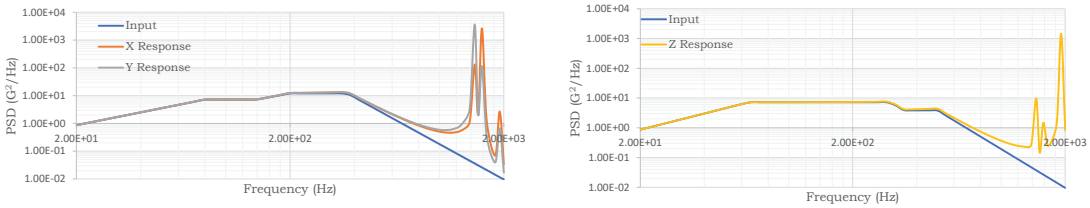

(a) (b)

Figure 5: Random vibration responses. Sub-figures (a) and (b) are the in plane response and out of plane response, respectively.

4 Concluding remarks

A systematic methodology for designing AM parts is conceptually presented in a step-by-step manner. Issues of communication between different softwares were considered and a solution was provided. Finally, the presented methodology is applied to a case study and some encouraging preliminary results of the topology optimization, part design (smoothing and part edition) and structural analysis stages are shown. The resultant design, compliant with the mass constraint, shows good behaviour in terms of stress and stiffness considering structural requirements only.

5 Future Work

In the short term, the engineering cycle of the LLM needs to be concluded. At this point, the engineering cycle of LLM considered structural requirements only. However, the work environment of an optomechanical part requires additional load cases and requirements. For instance, mechanical loading due to I/F tolerances and thermo-elastic loading due to the mismatch of thermal expansion coefficients. Finally, the process preparation and manufacturing campaign stages need to be also concluded. Moreover, the presented methodology is still in development and some key aspects are still missing. For instance, Ti6Al4V constitutive data (anisotropy, porosity and strength data) is missing, which shall be obtained from the ongoing experimental testing campaign. Additionally, fatigue testing campaign will be also performed in order to evaluate the probability of failure during launch. Finally, AM manufacturing constraints need to be added to the TO algorithm, namely the overhang constraints.

Acknowledgements

The authors gratefully acknowledge the financial support of the Portuguese Foundation for Science and Technology (FCT) under the projects CENTRO-01-0145-FEDER-029713 by UE/FEDER through the programs CENTRO 2020 and COMPETE 2020, and UID/EMS/ 00481/2013-FCT under CENTRO-01-0145-FEDER-022083. Financial support of program CENTRO 2020 and UE/FEDER is acknowledged through the project CENTRO-01-0247-FEDER-024039, designated as ADVANSS. B. Barroqueiro also acknowledges the financial support by the FCT through the scholarship SFRH/BD/120779/2016. The authors also acknowledge all the technical recommendations and revision cycles from OHB Systems at Oberpfaffenhofen.

References

[1] ISO International Standard. Additive manufacturing General principles Part 3: Main characteristics and corresponding test methods, 2014.

[2] Anders Clausen. *Topology Optimization for Additive Manufacturing*. PhD thesis, DTU Mechanical Engineering, Technical University of Denmark, 2016.

[3] Sebastian Kébreau, Dr. Patricia Cambrésy, André Dröse, Vincent Gröne, Kai Schimanski, and Freerk Syassen. Maturation of additive manufacturing for implementation into ariane secondary structures: Overview and status of "alm iscar". In *14th European Conference on Spacecraft Structures, Materials And Environmental Testing*.

[4] Gilles Pommatau, Florence Montredon, Antoine Carlino, Marion Salvi, Emmanuel Kot, Florence Clement, and Stephane Abed. Engineering design cycle for an additive layer manufactured secondary structure, from concept to final validation. In *Thales Alenia Space Comunication*.

[5] Aremu A, Ashcroft I, Hague R, Wildman R, and Tuck C. Suitability of SIMP and BESO Topology Optimization Algorithms for Additive Manufacture. *Wolfson School of Mechanical and Manufacuring Engineering*, 2010.

[6] MSC Software. MSC Nastran 2017.1: Design Sensitivity and Optimization User Guide, .

[7] M. P. Bendsøe. Optimal shape design as a material distribution problem. *Structural Optimization*, 1(4):193–202, dec 1989.

[8] C. Geuzaine and J.-F. Remacle. Gmsh: a three-dimensional finite element mesh generator with built-in pre- and post-processing facilities. *International Journal for Numerical Methods in Engineering*, 79(11):1309–1331, 2009.

[9] MSC Software. MSC Nastran 2017.1: Linear Static Analysis User Guide, .

[10] MSC Software. MSC Nastran 2017.1: Dynamic Analysis User Guide, .

[11] Michael Gouge and Pan Michaleris, editors. *Thermo-Mechanical Modeling of Additive Manufacturing*. Elsevier, 2018.

[12] ASTM International, West Conshohocken. ASTM WK47031: New Guide for Nondestructive Testing of Additive Manufactured Metal Parts Used in Aerospace Applications, 2014.

[13] ECSS E ST 10 03C. Space engineering: Testing, 2012.

[14] ASTM International, West Conshohocken. ASTM F3001-14, Standard Specification for Additive Manufacturing Titanium-6 Aluminum-4 Vanadium ELI (Extra Low Interstitial) with Powder Bed Fusion, 2014.